Long spatio-temporally stationary filaments in air using short pulse UV laser Bessel beams

D. Abdollahpour[1], P. Panagiotopoulos[1], M. Turconi[2,5], O. Jedrkiewicz[2,5], D. Faccio[2,5], P. Di Trapani[3,#], A. Couairon[4,5], D. G. Papazoglou [1,6], and S. Tzortzakis [1,*]

[1]*Institute of Electronic Structure and Laser (IESL), Foundation for Research and Technology – Hellas (FORTH), P.O. Box 1527, 71110 Heraklion, Greece*

[2] *CNISM and Department of Physics and Mathematics, University of Insubria, Via Valleggio 11, 22100 Como, Italy*

[3]*Department of Quantum Electronics, Vilnius University, Sauletekio Ave. 9, bldg.3, LT-10222, Vilnius*

[4]*Centre de Physique Théorique, CNRS, Ecole Polytechnique, F-91128, Palaiseau, France*

[5]*Virtual Institute for Nonlinear Optics, Centro di Cultura Scientifica Alessandro Volta, Villa Olmo, Via Simone Cantoni 1, 22100 Como, Italy*

[6] *Materials Science and Technology Department, University of Crete, P.O. Box 2208, 71003, Heraklion, Greece*

[#] *Permanent address: 2,5*

**e-mail: stzortz@iesl.forth.gr; http://unis.iesl.forth.gr*

Abstract: The formation of long stationary filaments resulting in uniform high density plasma strings in air using short pulse UV laser Bessel beams is shown. The length and the electron density of the plasma strings can be easily tuned by adjusting the conical Bessel wavefront angle. It is shown that in this regime the length of the plasma string can be extended over meter-long scales without any compromise in the string uniformity or any temporal evolution of the filamented laser pulse.

OCIS codes: (320.2250) Femtosecond phenomena; (320.7110) Ultrafast nonlinear optics; (350.5400) Plasmas; (280.5395) Plasma diagnostics

References and links

1. R. Ackermann, K. Stelmaszczyk, P. Rohwetter, G. Mejean, E. Salmon, J. Yu, J. Kasparian, G. Mechain, V. Bergmann, S. Schaper, B. Weise, T. Kumm, K. Rethmeier, W. Kalkner, L. Woste, and J. P. Wolf, "Triggering and guiding of megavolt discharges by laser-induced filaments under rain conditions," Appl. Phys. Lett. **85**, 5781-5783 (2004).
2. S. Tzortzakis, D. Anglos, and D. Gray, "Ultraviolet laser filaments for remote laser-induced breakdown spectroscopy (LIBS) analysis: applications in cultural heritage monitoring," Opt. Lett. **31**, 1139-1141 (2006).
3. G. Méjean, J. Kasparian, E. Salmon, J. Yu, J. P. Wolf, R. Bourayou, R. Sauerbrey, M. Rodriguez, L. Wöste, H. Lehmann, B. Stecklum, U. Laux, J. Eislöffel, A. Scholz, and A. P. Hatzes, "Towards a supercontinuum-based infrared lidar," Appl. Phys. B **77**, 357-359 (2003).
4. G. Méjean, J. Kasparian, J. Yu, S. Frey, E. Salmon, and J. P. Wolf, "Remote detection and identification of biological aerosols using a femtosecond terawatt lidar system," Appl. Phys. B **78**, 535-537 (2004).
5. C. P. Hauri, W. Kornelis, F. W. Helbing, A. Heinrich, A. Couairon, A. Mysyrowicz, J. Biegert, and U. Keller, "Generation of intense, carrier-envelope phase-locked few-cycle laser pulses through filamentation," Appl. Phys. B **79**, 673-677 (2004).
6. A. Zaïr, A. Guandalini, F. Schapper, M. Holler, J. Biegert, L. Gallmann, A. Couairon, M. Franco, A. Mysyrowicz, and U. Keller, "Spatio-temporal characterization of few-cycle pulses obtained by filamentation," Opt. Express **15**, 5394-5404 (2007).
7. R. W. Boyd, *Nonlinear Optics,* Second ed. (Academic Press, 2003), p. 578.
8. A. Couairon and A. Mysyrowicz, "Femtosecond filamentation in transparent media," Phys. Rep. **441**, 47-189 (2007).
9. P. Polesana, A. Couairon, D. Faccio, A. Parola, M. A. Porras, A. Dubietis, A. Piskarskas, and P. Di Trapani, "Observation of Conical Waves in Focusing, Dispersive, and Dissipative Kerr Media," Phys. Rev. Lett. **99**, 223902-223904 (2007).
10. D. Faccio, M. Clerici, A. Averchi, O. Jedrkiewicz, S. Tzortzakis, D. Papazoglou, F. Bragheri, L. Tartara, A. Trita, S. Henin, I. Cristiani, A. Couairon, and P. Di Trapani, "Kerr-induced spontaneous Bessel beam formation in the regime of strong two-photon absorption," Opt. Express **16**, 8213-8218 (2008).

#106828 - $15.00 USD Received 26 Jan 2009; revised 3 Mar 2009; accepted 3 Mar 2009; published 16 Mar 2009

11. C. L. Tsangaris, G. H. C. New, and J. Rogel-Salazar, "Unstable Bessel beam resonator," Opt. Commun. **223**, 233-238 (2003).
12. A. Vasara, J. Turunen, and A. T. Friberg, "Realization of general nondiffracting beams with computer-generated holograms," J. Opt. Soc. Am. A **6**, 1748-1754 (1989).
13. V. P. Koronkevich, I. A. Mikhaltsova, E. G. Churin, and Y. I. Yurlov, "Lensacon," Appl. Opt. **34**, 5761-5772 (1995).
14. P. Polesana, M. Franco, A. Couairon, D. Faccio, and P. Di Trapani, "Filamentation in Kerr media from pulsed Bessel beams," Phys. Rev. A **77**, 043814 (2008)
15. S. Akturk, B. Zhou, M. Franco, A. Couairon, and A. Mysyrowicz, "Generation of long plasma channels in air by focusing ultrashort laser pulses with an axicon," Opt. Commun. **282**, 129-134 (2009).
16. P. Polynkin, M. Kolesik, A. Roberts, D. Faccio, P. Di Trapani, and J. Moloney, "Generation of extended plasma channels in air using femtosecond Bessel beams," Opt. Express **16**, 15733-15740 (2008).
17. S. Tzortzakis, M. A. Franco, Y. B. André, A. Chiron, B. Lamouroux, B. S. Prade, and A. Mysyrowicz, "Formation of a conducting channel in air by self-guided femtosecond laser pulses," Phys. Rev. E **60**, R3505 (1999).
18. F. Chen, *Introduction to plasma physics and controlled fusion,* Second ed. (Springer, 2006).
19. D. G. Papazoglou and S. Tzortzakis, "In-line holography for the characterization of ultrafast laser filamentation in transparent media," Appl. Phys. Lett. **93**, 041120-041123 (2008).

1. Introduction

Numerous interesting laser-based applications, such as lightning control [1], remote LIBS [2], LIDAR [3, 4] or pulse compression [5, 6] depend on two key factors: the peak on axis laser intensity and the length over which this can be sustained. Evidently, such applications are strongly favored by the presence of a long path of high intensity, and consequently high electron density, in the propagation direction.

When the input laser pulse power is low its propagation is governed by the laws of linear optics. For instance, when a laser pulse is focused by a spherical lens the longitudinal length L of the focal region, known as the Rayleigh length, is $L \propto d^2$ while the intensity $I \propto 1/d^2$, where d is the focal spot diameter. Thus, in the linear regime any extension of the focal region is always in the expense of intensity. In contrary, when the laser pulse power exceeds the critical power for self focusing P_{cr} [7], a number of interesting nonlinear effects take place. One of the most exciting is filamentation, which corresponds to the self-organization of the laser beam in a small diameter intense mode that propagates over extended distances. This phenomenon can be qualitatively explained as a dynamical competition between linear and nonlinear effects including Kerr self-focusing, ionization defocusing, nonlinear losses and dispersion effects [8]. For typical Gaussian beams, focused by spherical lenses, filamentation extends on a region much longer than the Rayleigh length L while the intensity is maintained at very high levels (~ 10^{13} W/cm^2). Although filamentation seems a perfect candidate for the generation of long regions of high intensity there are also drawbacks. As mentioned already filamentation is a dynamical process with strong spatio-temporal effects that lead to a more or less modulated on axis distribution of intensity and plasma density. This modulation can somehow be moderated when the beam propagates in a medium exhibiting strong nonlinear absorption (two or three photon absorption), or when the high intensity peak is reached by means of a sufficiently smooth growth inside the nonlinear medium (adiabatic coupling) [9, 10].

On the other hand, filamentary-like propagation is also achievable, even in the linear propagation regime, by Bessel beams. Bessel beams can be viewed as the superposition of infinite plane waves whose wave-vector lies on a cone or as a superposition of two Hankel beams (see for example [11]). As this conical wave propagates, due to interference effects, an intense central core, surrounded by lower intensity rings is formed along the propagation direction. In the nonlinear regime the high intensity core of the Bessel beam will lead to the generation of free electrons through multi-photon ionization.

Bessel beams are commonly generated using axicons, while more complex optical systems such as holographic elements [12] and lensacons [13] can be used as well. An axicon is an optical element with one side flat and the other side conical. As the pulse propagates

#106828 - $15.00 USD Received 26 Jan 2009; revised 3 Mar 2009; accepted 3 Mar 2009; published 16 Mar 2009

through the axicon and exits from the conical side, the wavefront is transformed to conical. The total length of the Bessel zone depends on the input beam diameter and the axicon's conical angle.

Filamentation dynamics in various media using pulsed Bessel beams has already been studied (see [14], and references therein). More recently, ultrafast IR (800 nm) Bessel beams have been used to generate long plasma strings in air [15, 16]. In these works the reported simulated electron density values were in the range of 10^{16} cm^3. Furthermore, the plasma density was not uniform exhibiting either oscillations, due to the use of narrow beams and a blunt-tip axicon, [15] or significant variation over the propagation distance [16]. Also, it was reported [16] that by adding temporal chirp in the pulse, the plasma string position and length could be relatively extended but in the expense of peak electron density.

In this letter we report on the creation of tunable in length, uniform plasma strings of high electron densities (~ 10^{18} cm^{-3}) in air using UV short pulse Bessel beams. The use of UV radiation makes the ionization process very efficient and along with the optimization process achieved by the tuning of the Bessel beam angle makes it a perfect candidate for the generation of very long and uniform plasma strings in air. The string length tunability is achieved without sacrificing the plasma uniformity, while the impact on the peak electron densities is also very small.

2. Experimental setup

A hybrid feedback distributed dye/KrF excimer laser, delivering 0.5 ps (or 5 ps), 248 nm pulses was used in our study. The output laser beam profile was top-hat with spatial dimensions of 50-mm x 50-mm. The central part of the laser beam was selected by means of an iris and was directed towards the optical system that transformed the beam to conical. The optical system was either a simple fused silica axicon, with base angle of γ =5° (170° apex angle) or a system composed by the same axicon preceded by a fused silica plano-concave lens of f = -200 mm focal distance, placed 3 cm from the axicon, as shown in Fig. 1(a). In the experiments both available laser pulse modes, 0.5 ps and 5 ps, were used.

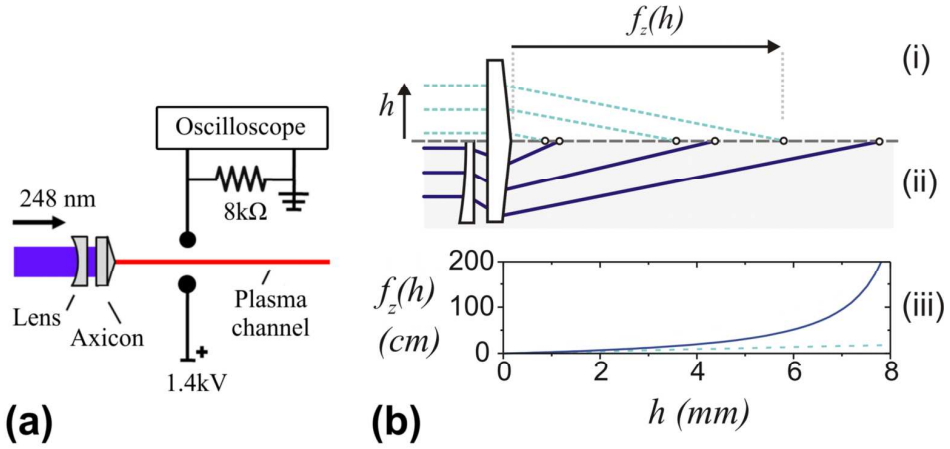

Fig. 1. (a) Experimental setup**.** (b) Ray tracing for (i) an axicon, (ii) an axicon preceded by a diverging lens. (iii) Axial focusing distance $f_z(h)$ as a function of the ray height h for an γ = 5° axicon (dashed line) and a combination of this axicon with a diverging lens (f = -200 mm) (solid line).

An electric conductivity technique was used to characterize the generated plasma strings after the axicon [17]**.** The measurement system consisted of two steel electrodes (~ 1 mm diameter) separated by 3 mm distance. A Teflon slit aperture was placed in front of the electrodes to exclude undesired ionization on the electrode's surfaces from the UV laser beam.

#106828 - $15.00 USD Received 26 Jan 2009; revised 3 Mar 2009; accepted 3 Mar 2009; published 16 Mar 2009

The plasma string passed between the two electrodes while a DC high voltage (1.4 kV) was applied on them. The laser generated plasma redistributed in the presence of the applied external electric field (~ 4.7 kV/cm) and screened out [18] the external field, generating a potential drop across the electrodes that caused a current to flow though the 8 kΩ probe resistance. The voltage drop across the resistance was measured using a standard oscilloscope. When this detection setup is operated in the ohmic regime (current is proportional to the applied high voltage) the measured electric signal depends linearly on the mean, over the plasma channel diameter, excited electron density $<N_e>$. The correlation of the electric conductivity measurements to plasma density estimations was done by comparison with a precise, but more complex, holographic method [19].

As mentioned above an axicon was used to generate the Bessel beam. From a ray tracing point of view an axicon focuses all the rays that lie on a cylinder of radius h to an axial focus at a distance $f_z(h)$ from the axicon apex, as shown in Fig. 1b(i). In contrast to a spherical lens the axial focus position depends linearly on the ray height h. For an axicon with small base angle the axial focus position can be written as: $f_z(h) \cong h/[(n-n_o)\gamma]$, where γ is the base angle of the axicon, n is the refractive index of the axicon and n_o is the refractive index of the surrounding medium (air). The longitudinal size of the focal region in this case is defined by the base angle of the axicon and the beam diameter. A highly efficient way to expand this region is to place a diverging lens before the axicon. The axial focusing range is expanded while the axial focus position is now a nonlinear function of the ray height h, as shown in Fig. 1b(ii). In this case with a good approximation the axial focus position can be written as:

$$f_z(h) \cong \frac{h}{(n-n_o)\gamma + h/f}, \tag{2}$$

where f is the focal distance of the diverging lens. It is clear that after the insertion of the diverging lens the optical system acts as an axicon with an effective base angle γ_{eff} given by:

$$\gamma_{eff} \cong \gamma + \frac{h}{f(n-n_o)} \tag{3}$$

The effective base angle is no longer constant and linearly depends on the ray height. Fig. 1b(iii) shows the significant extension of the longitudinal focusing range achieved by this approach.

3. Results and discussion

The electron density distributions of the plasma strings created when using the axicon alone are shown in Fig. 2(a) for both pulse durations. In both cases a homogeneous plasma channel ~ 150 mm long is created. The estimated electron density values are in the range of ~$2.5 \cdot 10^{18}$ cm^{-3} and $1 \cdot 10^{17}$ cm^{-3} for the 0.5 ps and 5 ps pulses respectively. The difference in the peak electron densities is due to the lower pulse intensity of the longer pulses.

Although homogeneous, the plasma strings obtained in this way are relatively short in length. To obtain longer plasma strings we introduced the diverging lens as described above. The obtained plasma string electron distributions are shown in Fig. 2(b), for the same input pulse parameters as in Fig. 2(a). One observes a considerable increase in the length of the plasma strings, without any compromise in the plasma uniformity, accompanied by a small reduction of the peak electron density. For the shorter 0.5 ps pulses the plasma string length was extended by a factor of ~10x with a ~3.4x reduction of the electron density (~ 7.4 10^{17} cm^{-3}). Despite this reduction, the plasma density is still 2 orders of magnitude higher than previously reported values from relative studies [15, 16]. Likewise, for the 5 ps pulses the plasma string length was increased by a factor of ~5x, accompanied with a ~2x reduction of the electron density values (~6 10^{16} cm^{-3}).

#106828 - $15.00 USD Received 26 Jan 2009; revised 3 Mar 2009; accepted 3 Mar 2009; published 16 Mar 2009

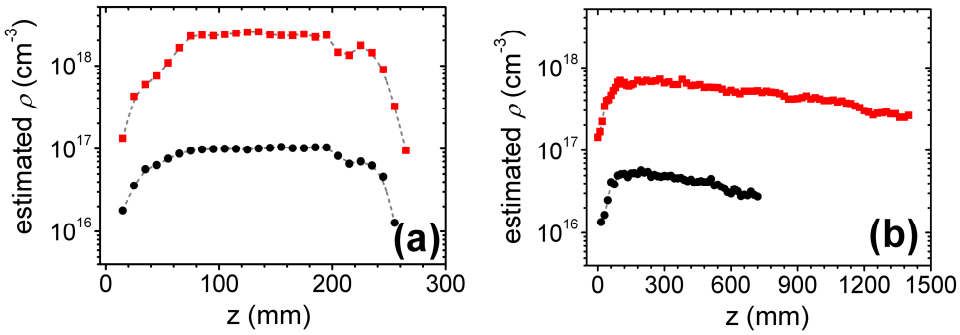

Fig. 2. Electron density ρ versus propagation distance for 248 nm, UV Bessel beams. (squares) - 7.5 mJ, 0.5 ps, (circles) - 10.25 mJ, 5 ps. (a) axicon only (base angle $\gamma = 5^{o}$), (b) axicon with diverging lens (f = -200 mm)

Beyond the spatially achieved stationarity we verified that this conically driven filamentary propagation does not involve any temporal effects either. For this we monitored the UV laser pulse spectrum before and after the formation of the plasma strings. The comparative spectra are shown in Fig. 3 for both pulse durations, showing insignificant spectral evolutions. This is a strong indication that no temporal effects, like pulse splitting, take place during the pulse propagation and plasma string formation.

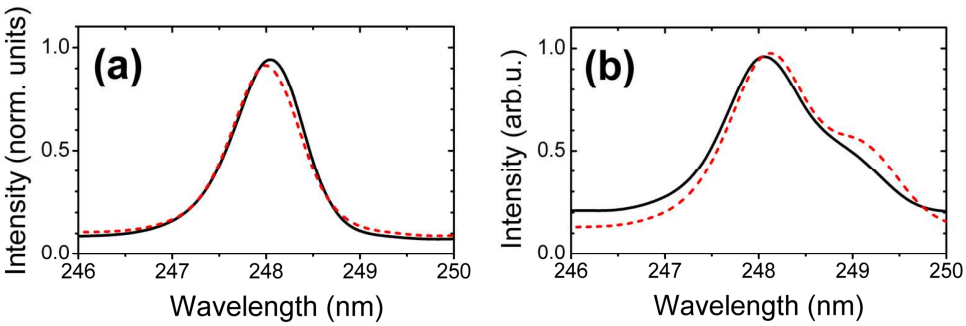

Fig. 3. The measured spectra of the pulse before (solid curve) and after (dashed line) formation of the plasma channel; (a) for 5 ps pulse duration and (b) for 0.5 ps pulse duration.

In order to further explore this conical filamentation regime numerical simulations of the nonlinear propagation have also been performed, using a complete 3D code that solves the nonlinear Schrödinger equation (NLSE) coupled with a rate equation for the electron density evolution. The numerical model is described in detail in [8] and it takes into account diffraction, plasma defocusing, group velocity dispersion by using the full dispersion relation (Sellmeir - like) for air, and nonlinear effects such as the Kerr effect, and multi photon absorption. The electron density evolution equation takes into account multi-photon ionization, as well as avalanche ionization and trapping. The effect of the axicon is modeled by the multiplication of the input field with a phase mask, $\exp[i\varphi(h)]$ where $\varphi(h) = -2\pi h \lambda^{-1} \sin[(n-1)\gamma]$, λ is the wavelength and n, γ are respectively the refractive index and the base angle of the axicon.

Simulations were performed under the same conditions as in the experiment (0.5 ps, 248 nm, axicon base angle $\gamma = 5^{o}$, diverging lens f =-200 mm). Furthermore, to clarify the role of nonlinear effects in the propagation we simulated two distinct cases: one for input energy of 7.5 mJ, as in our experiments, and one for very low, 7.5 nJ input energy (corresponding to a

#106828 - $15.00 USD Received 26 Jan 2009; revised 3 Mar 2009; accepted 3 Mar 2009; published 16 Mar 2009

power 7 10^{-5} P_{cr}) with all other parameters unchanged. The results of the simulation are shown in Fig. 4. As it is clear, the on-axis intensity for the low input energy is ~10^6 times smaller than the on-axis intensity, corresponding to the 10^6 times higher input energy, but follows the same shape as for the high input laser energy. This result confirms that the propagation is governed by the linear induced conical wavefront. The on-axis electron density, for the case of the 7.5 mJ input energy is also shown in Fig. 4. The peak electron density value of 6.5 10^{17} cm^{-3} of the simulation agrees nicely with the measured one 7.4 10^{17} cm^{-3}, while the simulated electron density is decaying faster as a function of the propagation distance. This discrepancy could be attributed to the fact that the electric conductivity technique, which is sensitive to the plasma string volume between the electrodes, results in averaged electron density values $<N_e>$, while the simulation results refer to the peak electron densities in the center of the plasma string core. Finally, the numerical results show no temporal evolution of the filamented laser pulses, in agreement with the experimental findings.

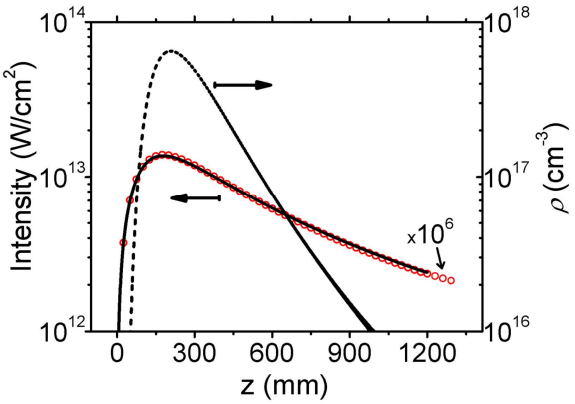

Fig. 4. Simulated on axis intensity and electron density profiles for 7.5 mJ, 248 nm, 0.5 ps pulses illuminating an axicon (base angle γ = 5°) preceded by a diverging lens (f = -200 mm). (solid line) – Intensity, (circles) –intensity values for 7.5 nJ pulses (x10^6), (dashed line)- on axis electron density

4. Conclusion

In conclusion, we have demonstrated that long, uniform and high density plasma strings can be generated in air using conically shaped UV short laser pulses. The combination of axicons with diverging lenses, actively tunes the conical angle, and results in a remarkable increase of the plasma string length with no sacrifice in the string uniformity and minimal peak electron density changes. Since the beam propagation is mainly governed by linear effects the propagation is stationary both in space and in time. These results could be scaled-up to higher input energies as the presence of strong nonlinear absorption would result to intensity clamping effects that would further flatten the intensity spatial profile, keeping the plasma density high over long propagation distances. Our approach is an attractive candidate for numerous applications like THz pulse generation or lightning control.

Acknowledgments

These results have been obtained in the context of the STELLA-2008 school (http://www.vino-stella.eu), held at the IESL-FORTH in Heraklion-Greece, in collaboration between the MC Chair project "STELLA" MEXC-CT-2005-025710 and the Marie Curie Excellence Grant "MULTIRAD" MEXT-CT-2006-042683 (http://unis.iesl.forth.gr). This work has also been supported by the European Commission Research Infrastructures "Laserlab-Europe" RII3-CT-2003-506350 (operating at the IESL-FORTH).

#106828 - $15.00 USD Received 26 Jan 2009; revised 3 Mar 2009; accepted 3 Mar 2009; published 16 Mar 2009